Origin of the Bismuth-Induced Decohesion of Nickel and Copper Grain Boundaries

Joongoo Kang, Greg C. Glatzmaier, and Su-Huai Wei

Phys. Rev. Lett. **111**, 055502 — Published 29 July 2013

DOI: 10.1103/PhysRevLett.111.055502

Origin of the Bismuth-Induced Decohesion of Nickel and Copper Grain Boundaries

Joongoo Kang, Greg C. Glatzmaier, and Su-Huai Wei

National Renewable Energy Laboratory, Golden, Colorado 80401, USA

Ductile metals such as Ni and Cu can become brittle when certain impurities (e.g., Bi) diffuse and segregate into their grain boundaries (GBs). Using first-principles calculations, we investigate the microscopic origin of the Bi-induced loss of cohesion of Ni and Cu GBs. We find that the Bi bilayer interfacial phase is the most stable impurity phase under Bi-rich condition, while the Bi monolayer phase is a metastable phase regardless of the value of the Bi chemical potential. Our finding is consistent with the recent experimental observation for Ni GBs [Luo *et al*., Science 333, 1730 (2011)]. The electric polarization effect of the Bi bilayer substantially enhances the strength of the Bi-metal interfacial bonds, stabilizing the bilayer phase over other phases. The Bi-Bi interlayer bonding is significantly weakened in the GBs, leading to a factor of 20 to 50 decrease in the GB cohesion, which has strong implications for the understanding of Bi-induced intergranular fracture of Ni and Cu polycrystals.

Metal embrittlement [1–18] is a complex phenomenon that involves nucleation and propagation of cracks as well as other dynamical effects [18,19]. It is well known that impurity-induced GB decohesion is an important mechanism of brittle failure of polycrystalline metals [3–5,11–14,17]. Bi-doped Ni and Cu have been investigated intensively as model systems for GB adsorption and embrittlement. There has been a debate on whether the Bi-induced decohesion of Cu GBs is caused by an electronic effect [11] (i.e., impurity-induced electronic structure changes) or a strain effect [12,13] associated with the large atomic size of Bi. Both studies assumed Bi sub- or monolayer phase in the GB models. A previous first-principles study [12] showed that the formation of Bi monolayer phase leads to a factor of 2 to 3 decrease in the work of separation of Cu GBs. However, a recent high-resolution scanning transmission electron microscopy (STEM) study by Luo *et al.* [14] showed that when Ni polycrystal is in contact with a Bi-Ni liquid alloy, the Bi impurity atoms diffuse into Ni GBs almost exclusively forming Bi bilayer phases in the GBs. This finding calls for a reappraisal of the Bi embrittlement mechanism of Cu and Ni based on the Bi monolayer models. Considering the relatively weak Bi-Bi interatomic bonding, which can be inferred from the low melting point of Bi metal [14], the formation of Bi bilayers may lead to the decohesion at the Ni GBs and associated GB embrittlement. It is, therefore, very important to understand the stability of various Bi impurity phases in metal GBs and the cohesion properties of these systems.

In this Letter, using density functional theory (DFT) calculations, we investigate various Bi impurity phases in Ni and Cu GBs as a function of the chemical potential of Bi (μ_{Bi}). We found that the Bi bilayer phase is the most stable impurity phase under Bi-rich condition, while the Bi monolayer phase is only a metastable phase in both Ni and Cu GBs, regardless of the value of μ_{Bi}. It was also shown that the Bi monolayer phase is thermodynamically unstable with respect to phase separation into a clean GB region and

another region with the Bi bilayer. More importantly, the Bi-Bi interlayer bonding in Bi bilayer phases is significantly weakened in the GBs, leading to a factor of 20 to 50 decrease in the GB cohesion. Consequently, the work of separation of Bi bilayers is an order-of-magnitude smaller than that of Bi monolayers. Thus, the decohesion of the GB region with the Bi bilayer may play an important role in Bi-induced embrittlement of Ni and Cu GBs.

To compare the stability of various adsorption phases with different Bi densities (ρ_{Bi}) in GB, we calculated the formation energy γ of an impurity phase as a function of μ_{Bi}. The γ per unit area is given by $\gamma = E(\text{GB:Bi}) - E(\text{GB}) - \rho_{Bi}\,\mu_{Bi}$. Here, E(GB:Bi) and E(GB) are the total energies per unit area of Bi-adsorbed GB and pure GB, respectively, which were calculated within the generalized gradient approximation (GGA-PBE [20]) to DFT, as implemented in the VASP package [21]. For Ni and Cu GB models, two representative types of GB structures, twist and tilt GBs, were considered (Supplemental Fig. S1 [22]). For twist GBs where the misorientation axis is normal to the fcc (111) GB plane, the following twist angles, $\theta_i = \cos^{-1}(\frac{3i^2+3i+0.5}{3i^2+3i+1})$, were chosen for integer i to make the upper and lower grains commensurate with the same lateral periodicity in our supercell calculations. For tilt GBs, we selected a symmetric 36.87° [001] tilt GB with $\Sigma = 5$.

In our model, Bi impurity atoms are incorporated into pure Ni GB as additional atoms, forming condensed Bi interfacial phases in the GBs in a Bi-rich condition. Three types of low-energy impurity phases—mono-, bi-, and trilayers of Bi atoms (denoted by ML, BL, and TL)—were identified in high-angle twist and tilt GBs of Ni [22]. For twist GBs with $\theta = 21.8°$, low- and high-density Bi impurity phases were identified with the atomic density per layer of 8.0 atoms/nm^2 and 10.6 atoms/nm^2, respectively [Figs. 1(a) and 1(b)]. We found that in both cases, the in-plane order of the Bi layer is a triangular lattice that is distorted from the ideal lattice, especially for the low-density phases, due to the Bi-Ni

bonds at the interface. For low-density Bi phases, the interfacial Bi-Ni bonds stabilize the triangular Bi lattice, which is otherwise unstable in a freestanding form (Supplemental Fig. S2). For BL, we found that both AB-like and AA-like stacks of Bi layers have almost the same formation energies. In the twist Ni GB, the AB-like stacking of BL_L (BL_H) is 0.004 eV/Å^2 (0.001 eV/Å^2) more stable than the corresponding AA-like stacking. Thus, we expect that the BLs with different stacking types can coexist in the GBs at high temperature, leading to an imperfect lattice-matching relationship between the upper and lower Bi layers [14]. For the tilt GB Σ5, we also identified the ML, BL, and TL [Fig. 1(c)]. Unlike the flat Bi layers in the twist GBs, the Bi layers of the BL in the tilt GB are conformed to the rough Ni grain surfaces, leading to the atomic-scale corrugation in the Bi layers.

Our atomic models of Bi BLs are consistent with the previous experimental result [14] in terms of the projected Bi-Bi distances (see Fig. 1) for the neighboring Bi columns within the same layer (d_{intra}) and for the neighboring Bi columns from the opposite layers (d_{inter}). From the STEM images, the d_{intra} is estimated to be d_{intra}(exp) ≈ 3.3 Å, which agrees well with the theoretical value d_{intra}(theory) = 3.28 Å for BL_L. The d_{intra} of BL_H is 2.85 Å, substantially smaller than the measured d_{intra}, indicating that BL_L better matches or represents the experimentally observed BLs. The d_{inter} of BL_L with AA-like stacking is d_{inter}(theory) = 3.89 Å, which agrees well with the experimental value, d_{inter}(exp) = 3.9 ± 0.6 Å. For the BL_L with AB-like stacking, the d_{inter} is 3.49 Å and 3.87 Å for the first and second neighboring Bi columns, respectively. Our TL_L model in Fig. 1(a), which has an atomically flat middle layer, is also consistent with the experimental TL structure that was observed as a metastable phase [14].

Figure 2(a) shows the γ of various Bi phases in the twist GB with $\theta = 21.8°$ as a function of chemical potential μ_{Bi} with the μ_{Bi} of bulk Bi phase as a reference, i.e., $\Delta\mu_{Bi} = \mu_{Bi} - \mu_{Bi}(\text{bulk})$. Although the γ was calculated from DFT calculations at zero temperature, the relative stability between the corresponding ML, BL, and TL, which consist of the same Bi layers as a building block, will not be altered much at finite temperature, because the entropy effect is largely cancelled out for these phases. The stability of Bi phases depends on μ_{Bi}. For $\Delta\mu_{Bi} < -0.17$ eV, ML_L is the most stable of the Bi interfacial phases. However, the γ of ML_L is a largely positive value, indicating that the clean GB is energetically more favored. For $\Delta\mu_{Bi} > -0.17$ eV, BL_L becomes a more stable phase than ML_L. So, ML is a metastable phase, regardless of the value of μ_{Bi}. At $\Delta\mu_{Bi} = 0.07$ eV, the excess energy necessary for the introduction of BL_L to the clean Ni GB is zero, suggesting that a first-order GB transition [23] between the clean GB and the BL may occur at the critical μ_{Bi}. As $\Delta\mu_{Bi}$ increases beyond 0.10 eV, the high-density phases, BL_H and TL_H, are stabilized in turn. In previous experiment [14], the Bi adsorption in GBs occurs in the Bi-rich condition in which Bi BL and Bi precipitates are in equilibrium in GBs. So μ_{Bi} should be close to or higher than $\mu_{Bi}(\text{bulk})$. At around $\Delta\mu_{Bi} = 0$, BL_L is the most stable of the Bi phases and thus the dominant interfacial phase, consistent with the experimental result [14].

So far, we have assumed the stress level in Ni GBs is nearly zero. However, a micrometer-scale crack usually exists at the surface of Ni polycrystal [14], and the liquid Bi atoms penetrate into the Ni bulk region through the crack until the penetrating liquid tip reaches the Ni GB region inside the sample. Then, the sharpness of the liquid tip induces large tensile stresses at the adjacent Ni GB, which can be relieved by the formation of BLs. Note that the γ of BL_L at $\Delta\mu_{Bi} = 0$ in Fig. 2(a) is small but positive ($\gamma = 0.011$ eV/Å^2). However, if the strain energy associated with the tensile stresses in Ni GB is taken into account, the γ of BL_L can be negative. Thus, the stress level at the GB needs to be large

enough for the BL formation with negative γ. Similarly, the tensile stress at a penetration front of the Bi BL inside the GB will promote the propagation of the BL front along GBs.

For tilt Ni GB Σ5, we found that the BL is the lowest-energy Bi interfacial phase with negative formation energy γ for -0.11 eV < $\Delta\mu_{Bi}$ < 0.14 eV [Fig. 2(b)], which indicates that in Bi-rich condition, Bi atoms can be easily incorporated into the tilt GB even at zero stress level. We also confirmed that the γ of the substitutional Bi atoms that occupy all the preferred atomic sites at the GB cores in Supplemental Fig. 1(b) [11] is higher than that of the BL for $\Delta\mu_{Bi}$ > -0.079 eV. The Bi incorporation with negative γ in Bi-rich condition is possible because the pure tilt GB Σ5 is a high-energy GB due to its large tilt angle. However, we expect that the BL formation and associated GB diffusion of Bi impurities will mainly occur in high-angle twist GBs, because the concentration of the tilt GB Σ5 in Ni polycrystal would be relatively low due to its large GB energy (0.078 eV/Å^2). This is consistent with our finding that the atomic structures of the BL_L and TL_L in twist GB models better match the experimental STEM images of Bi phases than in the tilt Σ5 GB.

For Cu-Bi, the stable GB phase changes in a sequence of clean GB, BL, and TL for high-angle twist GBs of Cu, as μ_{Bi} increases (Supplemental Fig. S3). This phase behavior is similar to that for Ni-Bi, except that the high-density Bi phases are more stable than the corresponding low-density phases in the twist Cu GB at $\Delta\mu_{Bi}$ = 0 due to the larger lattice constant of Cu than that of Ni. The BL is the most stable impurity phase with small γ at $\Delta\mu_{Bi}$ = 0, and thus expected to contribute to the Bi-induced embrittlement of Cu.

We have shown that the Bi BL in high-angle Ni and Cu GBs is more stable than the corresponding ML at $\mu_{Bi} = \mu_{Bi}$(bulk). A prior study [14] suggested that the ML is unstable due to the incoherent (or broken) bonds at one of the Bi-Ni interfaces. We note that the Bi

ML is less stable than the BL even for the twist angle $\theta = 0°$, in which the ML form coherent bonds both to upper and lower grains [24], indicating that in addition to the broken bond effect, a new mechanism is at work for the stabilization of BL. The relative stability of Bi interfacial phases can be understood in terms of the bond energies between different layers, $\Delta_{Ni\text{-}Ni}$, $\Delta_{Ni\text{-}Bi}$, and $\Delta_{Bi\text{-}Bi}$, at the GB. Here $\Delta_{Ni\text{-}Ni}$ refers to the bond energy per unit area between the two Ni layers at the pure Ni GB. The bond energy between the Ni surface layer and the Bi impurity layer is referred to as $\Delta_{Ni\text{-}Bi}$(BL) and $\Delta_{Ni\text{-}Bi}$(ML) for the BL and ML, respectively. $\Delta_{Bi\text{-}Bi}$ denotes the Bi-Bi interlayer bond energy of the BL. At $\mu_{Bi} = \mu_{Bi}$(layer), where μ_{Bi}(layer) is the μ_{Bi} of a *freestanding* Bi layer with the *same* geometry as in the GB-stabilized Bi phases, the formation energy of each phase can be expressed in terms of the bond energies; $\gamma(\text{ML}) = |\Delta_{Ni\text{-}Ni}| - 2|\Delta_{Ni\text{-}Bi}(\text{ML})|$ and $\gamma(\text{BL}) = |\Delta_{Ni\text{-}Ni}| - 2|\Delta_{Ni\text{-}Bi}(\text{BL})| - |\Delta_{Bi\text{-}Bi}|$. We found that $\Delta_{Bi\text{-}Bi}$ is relatively small ($\Delta_{Bi\text{-}Bi} \approx -0.01$ eV/Å^2). If we assume $|\Delta_{Ni\text{-}Bi}(\text{ML})| \approx |\Delta_{Ni\text{-}Bi}(\text{BL})|$, the formation energies of the ML and BL would be nearly the same at $\mu_{Bi} = \mu_{Bi}$(layer). In this case [Fig. 3(a)], the ML becomes more stable than the BL at $\mu_{Bi} = \mu_{Bi}$(bulk), because μ_{Bi}(bulk) is much smaller than μ_{Bi}(layer). So the Bi-Ni bond strength for the BL should be sufficiently larger than for the ML to stabilize the BL over the ML at $\mu_{Bi} = \mu_{Bi}$(bulk) [Fig. 3(b)]. For example, for the low-density Bi phases in Fig. 1(a) with μ_{Bi}(layer) = μ_{Bi}(bulk) + 1.0 eV, the difference in the Ni-Bi bond energy should be $|\Delta_{Ni\text{-}Bi}(\text{BL})| - |\Delta_{Ni\text{-}Bi}(\text{ML})| > 0.034$ eV/Å^2 for $\gamma(\text{BL}) < \gamma(\text{ML})$ at $\mu_{Bi} = \mu_{Bi}$(bulk). Indeed, our calculations show that $\Delta_{Ni\text{-}Bi}(\text{ML}) = -0.13$ eV/Å^2 and $\Delta_{Ni\text{-}Bi}(\text{BL}) = -0.17$ eV/Å^2, giving the bond-strength difference of 0.041 eV/Å^2.

The plot of the charge density difference associated with the Ni-Bi bond formation for BL reveals that the interfacial bonds induce an electric dipole at each Bi atom in the BL [Fig. 3(c)], which has a different direction depending on which Bi layer the atom belongs to. By forming the atomic dipoles at the Bi atoms, the Bi-Ni bond strength becomes

enhanced due to the Coulomb attraction between the positively charged pockets at the Bi atoms and the negatively charged regions between the Bi and Ni layers. In contrast, such an atomic dipole does not exist for the case of the ML due to the symmetric Ni-Bi bond configuration with respect to the Bi layer in the middle [Fig. 3(d)]. As a result, the Coulomb attraction associated with the atomic dipoles is absent in the ML, leading to 24% smaller $|\Delta_{Ni\text{-}Bi}|$ for the ML than for the BL. This bond-strength difference stabilizes the BL over the ML in Ni and Cu GBs in the Bi-rich condition.

Finally, we discuss how the formation of Bi interfacial phases in Ni GBs affects the adhesive property of Ni GB. The ideal work of separation W_∞ of a Bi BL in Ni GB, defined as the minimum energy needed to separate the interface into two free ML surfaces with the same crystallographic orientation [25], was calculated (see Supplemental Fig. S4). The W_∞ of the BL_L in the twist GB with $\theta = 21.8°$ is found to be 0.16 J/m^2, which is only 5% of that of the pure Ni twist GB (W_∞ = 3.18 J/m^2). The loss of cohesion in the GB-stabilized BL is general in all BL models; W_∞ = 0.11 J/m^2 for the BL_H in the high-angle twist GB and W_∞ = 0.08 J/m^2 for the BL in the tilt GB $\Sigma5$. For comparison, the W_∞ of the *freestanding* BL_L is calculated using the *same* atomic positions as in the BL_L in the high-angle twist GB. We found that the W_∞ of the freestanding BL_L is 0.95 J/m^2, which is substantially larger than that of the GB-stabilized BL_L. This clearly indicates that the Bi-Bi interlayer bonds are much weakened when strong Bi-Ni bonds form at the interfaces. Consequently, the W_∞ of Bi BLs are an order-of-magnitude smaller than the critical energy release rate (1–2 J/m^2) of strained GBs through dislocation nucleation [12,16] and plastic deformation. Thus, the Bi-incorporated Ni polycrystals become susceptible to intergranular fracture.

In conclusion, our DFT calculations show that in Ni and Cu GBs, the Bi BL is the most stable and thus the dominant interfacial phase in a Bi-rich condition. The significantly

weakened Bi-Bi interlayer bonds in Bi BL are responsible for the 95% to 98% reduction of cohesion at the metal GBs. Although the enormous reduction in cohesion has implications for Bi-induced intergranular fracture, it will require atomistic simulations of the fracture process to fully understand the role of the Bi BLs and associated GB decohesion in Bi-induced brittle failure of Ni and Cu. Thus, our finding will stimulate further studies of impurity phases in GBs in other material systems beyond the classical Langmuir-McLean-type adsorption models [14] and impurity-induced embrittlement mechanisms of metal GBs.

After the manuscript submission, we learned about a recent experimental paper [26] reporting on the observation of Bi bilayer phases in faceted segments of Cu GBs, which is consistent with our DFT results of Cu-Bi systems.

Acknowledgement. This work was funded by the U.S. Department of Energy's EERE CSP Program (DE-AC36-08GO28308). This research used the capabilities of the NREL CSC (DE-AC36-08GO28308) and the NERSC (DE-AC02-05CH11231).

1. B. Joseph, M. Picat, and F. Barbier, Eur. Phys. J. Appl. Phys. **5**, 19 (1999).

2. P. J. L. Fernandes, R. E. Clegg, and D. R. H. Jones, Eng. Failure Anal. **1**, 51 (1994).

3. R. C. Hugo amd R. G. Hoagland, Scripta Mater. **38**, 523 (1998).

4. W. Sigle, G. Richter, M. Rühle, and S. Schmidt, Appl. Phys. Lett. **89**, 121911 (2006).

5. W. Ludwig, E. Pereiro-López, and D. Bellet, Acta Mater. **53**, 151 (2005).

6. K. Wolski and V. Laporte, Mater. Sci. Eng., A **495**, 138 (2008).

7. B. Joseph, F. Barbier, and M. Aucouturier, Scripta Mater. **40**, 893 (1999).

8. U. Alber, H. Müllejans, and M. Rühle, Acta Mater. **47**, 4047–4060 (1999).

9. K. Ina and H. Koizumi, Mater. Sci. Eng., A **387–389**, 390 (2004).

10. R. Wu, A. J. Freeman, and G. B. Olson, Science **265**, 376 (1994).

11. G. Duscher, M. F. Chisholm, U. Alber, and M. Rühle, Nat. Mater. **3**, 621 (2004).

12. R. Schweinfest, A. T. Paxton, and M. W. Finnis, Nature **432**, 1008 (2004).

13. A. Y. Lozovoi, A. T. Paxton, and M. W. Finnis, Phys. Rev. B **74**, 155416 (2006).

14. J. Luo, H. Cheng, K. M. Asl, C. J. Kiely, and M. P. Harmer, Science **333**, 1730 (2011).

15. M. P. Harmer, Science **332**, 182 (2011).

16. P. M. Anderson and J. R. Rice, Scripta Metall. **20**, 1467–1472 (1986).

17. M. Yamaguchi, M. Shiga, and H. Kaburaki, Science **307**, 393–397 (2005).

18. H.-S. Nam and D. J. Srolovitz, Phys. Rev. Lett. **99**, 025501 (2007).

19. R. J. Zamora, A. K. Nair, R. G. Hennig, and D. H. Warner, Phys. Rev. B **86**, 060101 (2012).

20. J. P. Perdew, K. Burke, and M. Ernzerhof, Phys. Rev. Lett. **77**, 3865–3868 (1996).

21. G. Kresse and J. Furthmüller, Phys. Rev. B **54**, 11169–11186 (1996).

22. See Supplemental Material at http://link.aps.org/supplemental/... for details on the calculation method and supplemental figures.

23. S. Ma, K. M. Asl, C. Tansarawiput, P. R. Cantwell, M. Qi, M. P. Harmer, and J. Luo, Scripta Mater. **66**, 203–206 (2012).

24. For $\theta = 0°$, the γ of the BL_L at $\Delta\mu_{Bi} = 0$ is 0.012 eV/Å^2 lower than that of the ML_L.

25. T. E. Jones, M. E. Eberhart, S. Imlay, C. Mackey, and G. B. Olson, Phys. Rev. Lett. **109**, 125506 (2012).

26. A. Kundu, K. M. Asl, J. Luo, and M. P. Harmer, Scripta Mater. **68**, 146–149 (2013).

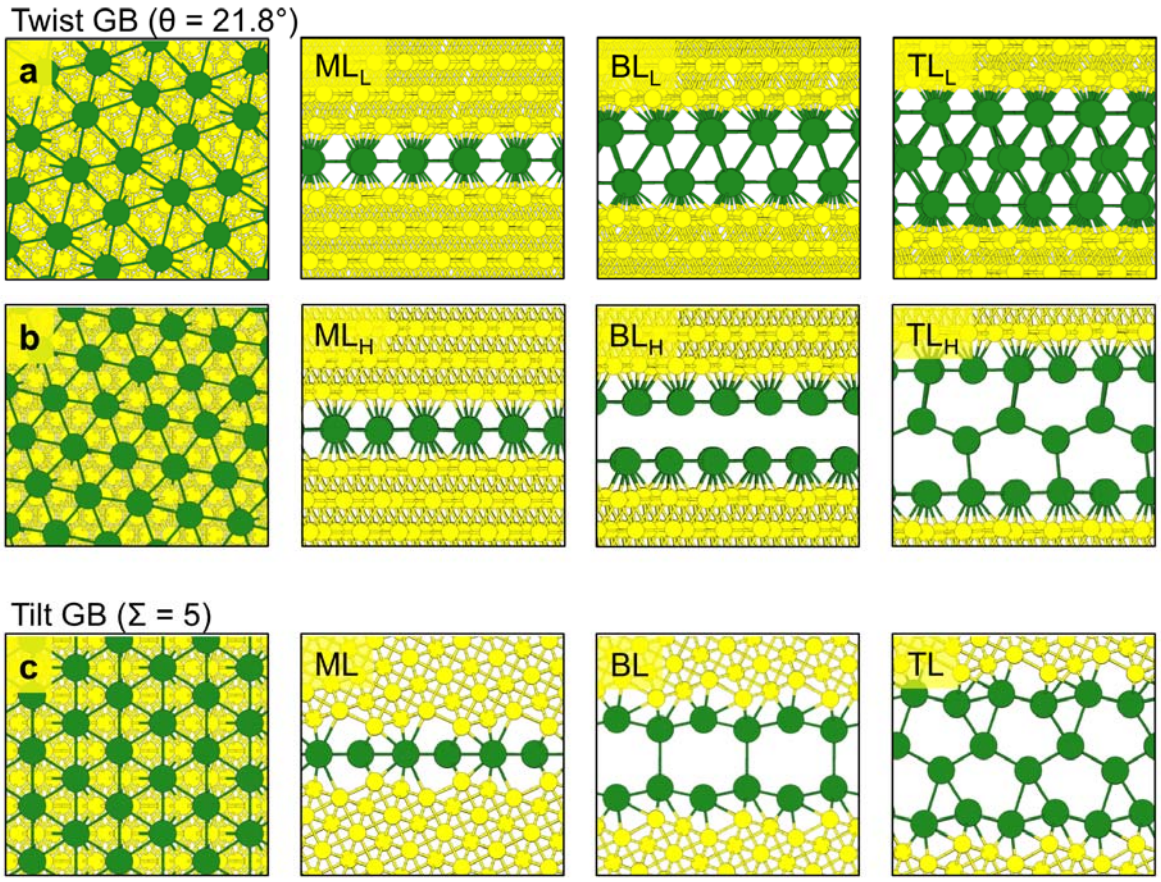

FIG. 1 (color online) The Bi interfacial phases in (a–b) high-angle twist GB with θ = 21.8° and (c) high-angle tilt GB Σ5. The subscripts L and H in (a–b) denote the low- and high-density Bi phases, respectively. In each row of the atomic structures (Ni is yellow and Bi is green), we present the in-plane structure of a single Bi impurity layer adsorbed on the GB plane and the corresponding Bi ML, BL, and TL phases.

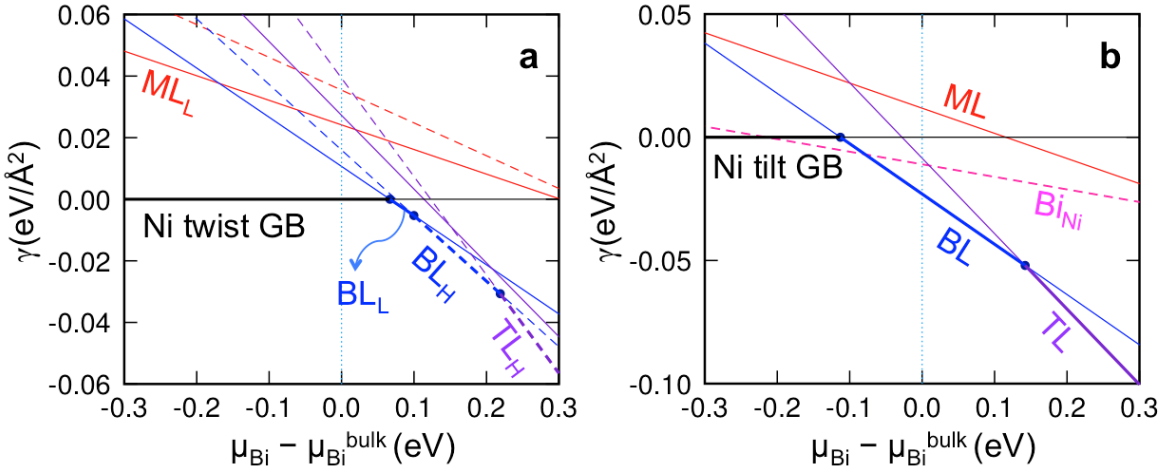

FIG. 2 (color online) (a) Formation energies γ of Bi interfacial phases in twist GBs with θ = 21.8° as a function of the chemical potential of Bi (μ_{Bi}). The solid lines are the results for the low-density Bi phases in Fig. 1(a), and the dashed lines are for the high-density Bi phases in Fig. 1(b). The slope becomes steeper with the increasing number of Bi layers from one to three. (b) Same as in (a), but for tilt GB with Σ = 5. The dashed line is the result for the Bi-segregated tilt GB (denoted by Bi_{Ni}) in which Bi impurities substitute for Ni atoms on the preferred atomic sites in the GB cores.

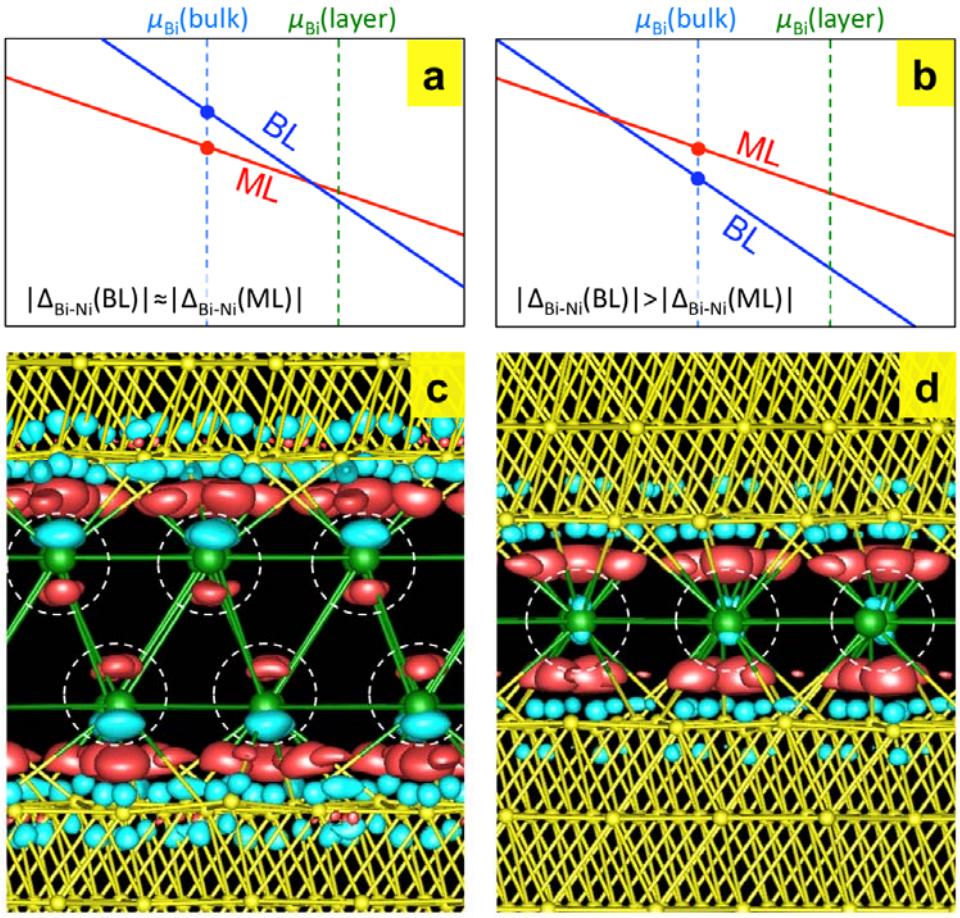

FIG. 3 (color online) Schematic of the relative stability of the Bi ML and BL in Ni GB as a function of the Bi chemical potential (μ_{Bi}) for (a) $|\Delta_{Ni\text{-}Bi}(BL)| \approx |\Delta_{Ni\text{-}Bi}(ML)|$ and (b) $|\Delta_{Ni\text{-}Bi}(BL)| > |\Delta_{Ni\text{-}Bi}(ML)|$, where $\Delta_{Ni\text{-}Bi}$ refers to the bond energy between the Ni and Bi layers at the GB. (c) The calculated electron charge density difference for the Bi BL_L in the Ni twist GBs with $\theta = 21.8°$. The charge density difference is given by $\Delta\rho_e(BL) = \rho_e(GB{:}BL) - \rho_e(GB) - \rho_e(ML_{upper}) - \rho_e(ML_{lower})$, where $\rho_e(GB)$, $\rho_e(ML_{upper})$, and $\rho_e(ML_{lower})$ are the charge densities for the isolated GB with the same atomic positions as in the GB:BL and the freestanding upper and lower Bi layers, respectively. The contour surfaces are plotted for $\Delta\rho_e = -0.044\ |e|/Å^3$ (red) and $\Delta\rho_e = 0.044\ |e|/Å^3$ (blue). (d) Same as (c), but for the ML_L and $\Delta\rho_e(ML) = \rho_e(GB{:}ML) - \rho_e(GB) - \rho_e(ML)$.